

Vertically Stacked Color Tunable Light-Emitting Diodes Fabricated Using Wafer Bonding and Transfer Printing

Jaeyi Chun,[†] Kwang Jae Lee,[‡] Young-Chul Leem,[‡] Won-Mo Kang,[‡] Tak Jeong,[§] Jong Hyeob Baek,[§] Hyung Joo Lee,[#] Bong-Joong Kim,[‡] and Seong-Ju Park^{*,†,‡}

[†]Department of Nanobio Materials and Electronics and [‡]School of Materials Science and Engineering, Gwangju Institute of Science and Technology, Gwangju 500-712, Republic of Korea

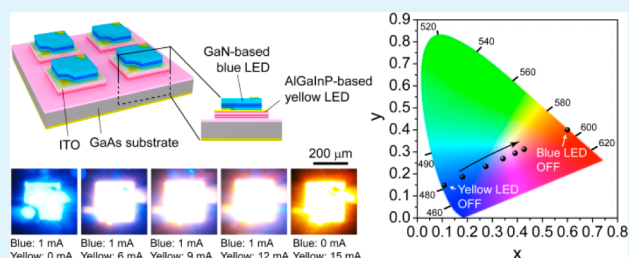
[§]LED Device Research Center, Korea Photonics Technology Institute, Gwangju 500-779, Republic of Korea

[#]CF Technology Division, AUK Corporation, Iksan 570-210, Republic of Korea

Supporting Information

ABSTRACT: We report on the vertically stacked color tunable light-emitting diodes (LEDs) fabricated using wafer bonding with an indium tin oxide (ITO) layer and transfer printing by the laser lift-off process. Employing optically transparent and electrically conductive ITO as an adhesion layer enables to bond the GaN-based blue and AlGaInP-based yellow LEDs. We find out that the interdiffusion of In, O, and Ga at the interface between ITO and GaP allows the strong bonding of the heterogeneous optoelectronic materials and the integration of two different color LEDs on a single substrate. The efficacy of this method is demonstrated by showing the successful control of color coordinate from the vertically stacked LEDs by modulating the individual intensity of blue and yellow emissions.

KEYWORDS: color tunable light-emitting diodes, vertical integration, ITO adhesion layer, wafer bonding, transfer printing



Inorganic light-emitting diode (LED) has been focused as a key component in solid-state lighting source because of its intrinsic properties such as high internal quantum efficiency (IQE), external quantum efficiency, low power consumption, and long-term stability.^{1–3} Numerous efforts in past decade have significantly developed the LED technology to satisfy the diverse requirements for solid-state lighting systems including general lighting and outdoor digital signage.^{4,5} Charge separation in a GaN-based active region which reduces the IQE has been improved using staggered quantum well structures^{6,7} and nonpolar or semipolar GaN LEDs.^{8,9} Epitaxial lateral overgrowth (ELOG) and surface plasmon have been also managed to increase the IQE,^{10,11} and surface texturing or photonic crystal have been suggested for high light extraction efficiency.^{12,13}

In addition, previous studies have introduced methods to fabricate passive or active matrix monochromatic microdisplays using GaN-based blue or green LEDs.^{14–17} These addressing techniques show the feasibility for use in next-generation visual systems that are high resolution, near-to-eye, or for projections. However, different structural aspects between GaN-based LEDs covering from blue to green and AlGaInP-based LEDs emitting in the range from yellow to red make it difficult to grow and integrate both materials on a same substrate.¹⁸ Current skills to generate multicolor LEDs through the mechanical packaging of different color LED chips in a lateral configuration impose a limit on the resolution due to chip placement accuracy which is

a few hundred microns.¹⁷ Therefore, the problematic issue of integrating red, green, and blue primary color LEDs on a single wafer should be challenged to expand its applications to high-resolution full-color compact displays, biomedical, and optogenetic applications which require multiwavelengths for in vivo or in vitro illumination of biological units located on tiny area.¹⁹ Previously, several studies have suggested approaches to fabricate single wafer-based color tunable LEDs using multifaceted GaN nanorods,²⁰ high In-content InGaN-based LEDs,²¹ and inkjet printing of organic color converters on ultraviolet LEDs,²² but the external bias-dependent color change and the degradation of emission efficiency because of color converters still require breakthroughs to achieve full range color tunability by controlling the emission intensity of the primary colors.

Here, we report color tunable dual wavelength LEDs by vertically stacking GaN-based blue LEDs onto AlGaInP-based yellow LEDs using wafer bonding and transfer printing processes. This scheme not only enables the construction of heterogeneous materials on a single substrate for compact pixel design using a simple fabrication process, but also provides a wide range of color control by modulating the individual intensity of highly pure blue and yellow emission. The bonding

Received: August 12, 2014

Accepted: November 3, 2014

Published: November 3, 2014

and transfer printing techniques provide a straightforward pathway to produce high-efficiency LEDs in a lattice mismatching system,^{23,24} vertical LED chips for high thermal and electrical performance,^{25,26} and flexible LED devices for various shape deformations.^{27–29} However, there were no reports on color tunable inorganic LEDs by integrating inhomogeneous materials on a single wafer using the bonding and transfer printing technology. The key strategy to this approach was to employ optically transparent and electrically conductive indium tin oxide (ITO) as an adhesion layer between blue and yellow LEDs which had a high efficiency of emission. Even though a few studies have reported that transparent conducting materials such as ITO or ZnO can be bonded to InGaAs or GaN layer using wafer fusion at high temperatures,^{30,31} their ability to bond GaN-based LEDs and AlGaInP-based LEDs has not been investigated. To demonstrate the efficacy of this method, we show the electroluminescence (EL) emission from the GaN-based blue and AlGaInP-based yellow LEDs that were vertically stacked using an ITO bonding layer and control the color coordinate on an International Commission on Illumination (CIE) 1931 x - y chromaticity diagram by adjusting the injection current in each LED.

Figure 1a presents a schematic describing the fabrication of the vertically stacked color tunable LEDs using wafer bonding to the ITO adhesion layer and transfer printing with the laser lift-off (LLO) process. We grew a GaN-based InGaInP/GaN multiple quantum well (MQW) LED epilayer on sapphire for blue emission (480 nm) and an AlGaInP-based LED epilayer on GaAs for yellow emission (590 nm) using metalorganic chemical vapor deposition (MOCVD) (see Figure S1 in the Supporting Information for detailed structures of the GaN-based blue and the AlGaInP-based yellow LEDs). The complementary colors of blue and yellow were selected to achieve coordinates on CIE x - y chromaticity diagram in the white region. First, an 800 nm thick ITO adhesion layer was deposited on top of the GaN-based epilayer by electron beam (e-beam) evaporation of a compound source of In₂O₃ (90 wt %) and SnO₂ (10 wt %), followed by a rapid thermal annealing process for ITO at 500 °C for 1 min. After bringing the two top planes (the ITO of the blue LED and the GaP of the yellow LED) in contact, wafer fusion bonding was carried out at 600 °C for 4 h under a weight pressure of 2.2 MPa. Just before the wafer fusion process, the surfaces of both samples were cleaned and the samples were directly stacked since the surface cleanliness of the LED wafers is crucial in fusion bonding.³² The bonding temperature of 600 °C used for an ITO adhesion layer was low enough to avoid the thermal stress on MQW layers. This is important because the optical performance of LEDs could be degraded during an annealing process at high temperatures.³³ Afterward, the blue LED epilayer was separated from the sapphire substrate using a KrF excimer laser. The transferred blue LED layer onto AlGaInP-based yellow LED layer as shown in Figure 1b demonstrates that the bonding between the ITO and the GaP is strong enough to allow an LLO process without delamination of the ITO bonding layer (see Figure S2 in the Supporting Information for detailed chemical structures of the bonding interface after the bonding process). The vertically stacked configuration using the bonding and transfer printing process shown in Figure 1c provides a stable platform to integrate different color LEDs on the same substrate and it can reduce the area of microsize LED pixels for high-resolution displays compared to the conven-

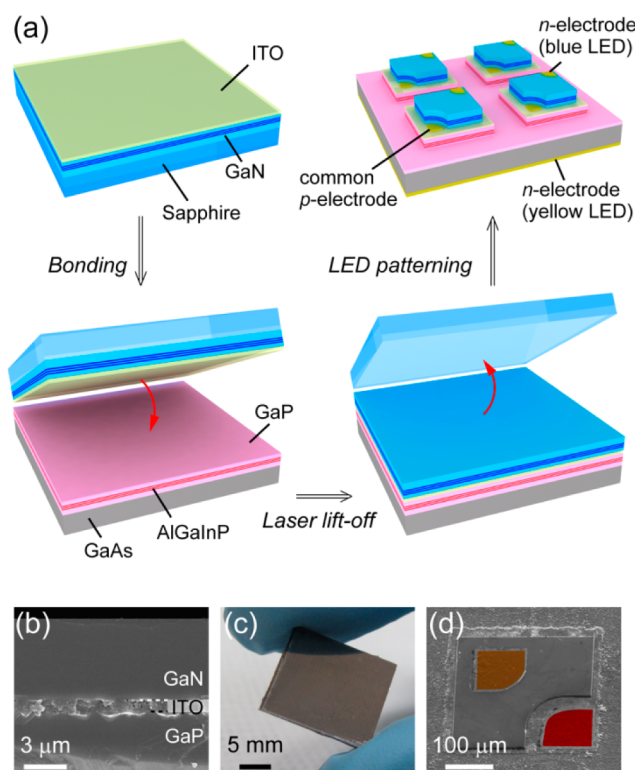


Figure 1. (a) Illustration of the fabrication steps to generate color tunable LEDs using wafer bonding and transfer printing. (b) Cross-sectional SEM image of the ITO adhesion layer. (c) Photograph of GaN-based blue LED film that was transferred onto the AlGaInP-based yellow LED epilayer. The sample size was 1.5×1.5 cm². This platform provides a stable way to integrate blue and yellow LEDs in a vertically stacked configuration. (d) Tilted SEM image of the integrated blue and yellow LEDs in a vertically stacked configuration after completion of the fabrication process. The orange is the n-electrode of the blue LED, and the red is the common p-electrode of the blue and yellow LEDs.

tional lateral configuration of LED pixels. We believe that the integration scheme of heterogeneous photonic materials by using an ITO adhesion layer can be also used for other optoelectronic devices such as photodetectors, solar cells, and laser diodes.

Inductively coupled plasma-reactive ion etching (ICP-RIE) and e-beam evaporation of Ti/Au were used to produce the blue LED pixels and the electrodes through the photolithographically defined masks (see Figure S3 in the Supporting Information for the LED pixelation process). Figure 1d shows the top view of the color tunable LEDs. The n-electrode for the blue LED is shown in orange on top of the architecture and the red electrode on the exposed ITO region is the common p-electrode for the blue and yellow LEDs. The transfer printing process induces the inverted shape of the GaN-based LED, resulting in an ITO-inserted n-p-n structure to be operated by three terminals (the n-electrode for the AlGaInP-based yellow LED is not shown in the figure). The three terminals (the two terminals on the top and one terminal at the bottom) can decrease the size of the color tunable LEDs by simplifying the wire bonding.

To investigate the chemical structure of the bonding interface between ITO and GaP, we prepared a partially bonded sample at a slightly lower bonding temperature of 550 °C and a shorter bonding time of 5 min. The mildly bonded

sample was then mechanically separated at the interface between the ITO and the GaP. The morphology of the surfaces of GaP and ITO was inspected using scanning electron microscopy (SEM) as shown in Figure 2a, b. The small bright

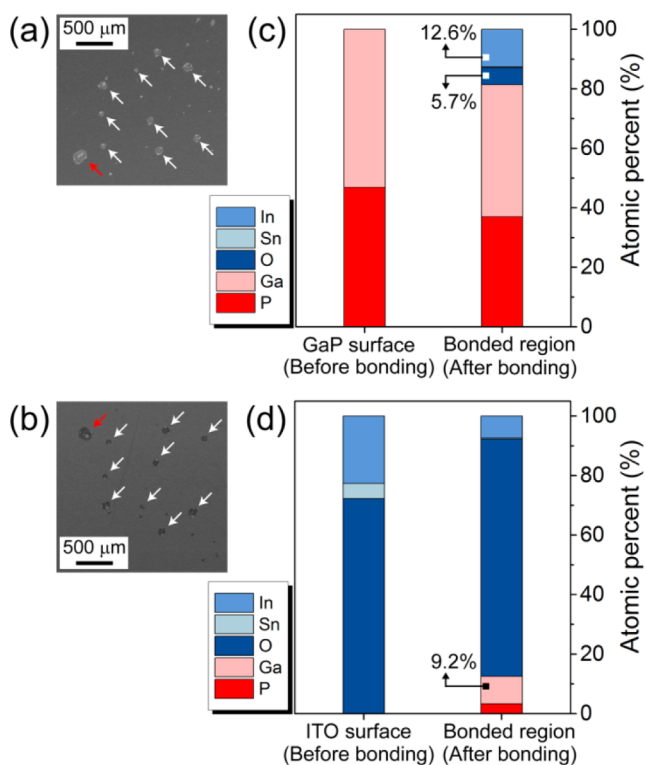


Figure 2. (a) SEM image of the separated GaP surface after mild bonding at 550 °C for 5 min. The arrows indicate the bonded regions. (b) SEM image of the separated ITO surface corresponding to the same area as in a. (c) Relative atomic composition measured using EDX spectroscopy of In, Sn, O, Ga, and P on the GaP surface before bonding (left bar) and the bonded region indicated by the red arrow in (a) after bonding (right bar). (d) Relative atomic composition measured using EDX spectroscopy on the ITO surface before bonding (left bar) and the bonded region indicated by the red arrow in b after bonding (right bar).

spots in the round shape indicated by the arrow on the separated GaP and ITO surfaces in Figure 2a, b represent the bonded regions formed at the initial stage of the bonding process. The random distribution of the bonded regions indicates that the bonding would start from more reactive sites at the interface between the ITO and GaP layer. The atomic composition of the bonded region on the surface of the separated ITO and GaP was investigated using energy-dispersive X-ray (EDX) spectroscopy to examine the change in the chemical composition of the surfaces before and after wafer bonding. We measured the EDX peaks of In, Sn, O, Ga and P from one of the bonded regions on the GaP and ITO surfaces (indicated by the red arrow in Figure 2a, b) and compared the peaks with the atomic composition of the GaP and the ITO surface before bonding (see Figure S4 in the Supporting Information for the EDX spectra). As shown in Figure 2c, the EDX analysis shows that the bonded region on the GaP surface has 12.6% In and 5.7% O, whereas the GaP surface before bonding had no In or O. Also, the bonded region on the separated ITO surface had 9.2% Ga composition, as

shown in Figure 2d. These results imply that In, O, and Ga are associated with the bonding process.

Previous reports on Ohmic contacts between ITO and Ga-V compound semiconductors have suggested the interdiffusion of In/Sn/O and Ga at the interface.^{34–36} Auger electron spectroscopy depth profiling of the interface region showed that In/O and Ga diffuse during annealing at 435 °C, generating a mixed phase of $\text{In}_x\text{Ga}_y\text{O}_z$ at the interface between GaP and ITO.³⁶ We also believe that the EDX peaks of In and O on the GaP surface and Ga on the ITO surface, as shown in Figure 2c and d, can be attributed to the mixed interfacial layer composed of In–Ga–O through diffusion at the ITO/GaP bonding interface. Therefore, fusion bonding of blue and yellow LEDs with an ITO interlayer at a higher temperature of 600 °C for 4 h could enhance the diffusion of the elements to generate a mixed interfacial layer that would enable strong bonding of ITO and GaP.

Figure 3a shows the EL spectra of individually operated blue and yellow LEDs in the vertically stacked configuration. Here, we evaluated the optical properties of the LEDs at low injection currents because the low optical output power of LEDs would be sufficient for various applications such as displays and

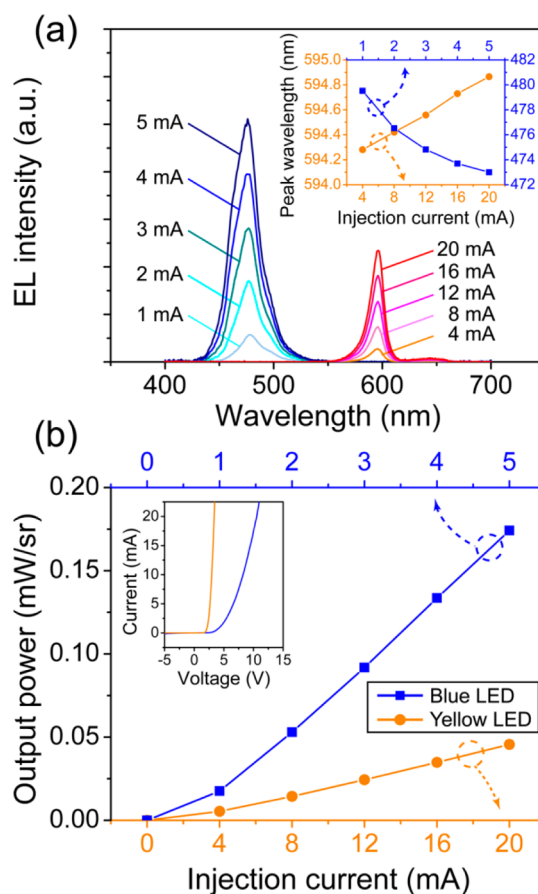


Figure 3. (a) Representative EL spectra from the individually operated GaN-based blue (left) and AlGaInP-based yellow LED (right) at various injection currents. The inset shows the peak wavelength change of the blue (blue line with solid squares) and the yellow (orange line with solid circles) LEDs as a function of the injection current. (b) Representative $L-I$ characteristics of the blue (blue line with solid squares) and yellow (orange line with solid circles) LEDs. The inset shows the $I-V$ properties of blue (blue line) and yellow (orange line) LEDs.

medical applications^{16,37} (see Figure S5 in the Supporting Information for the stability of the vertically stacked LEDs at high driving currents). The peak wavelength of the blue LED was blue-shifted by 6.5 nm from 479.5 to 473.0 nm as the injection current increased from 1 mA to 5 mA. It is believed that the band filling and screening of the quantum confined Stark effect are the main causes of the blue-shift in GaN-based LEDs.³⁸ The yellow LEDs had emission peaks that were red-shifted by 0.6 nm (from 594.3 to 594.9 nm) at an injection current of 20 mA. Since there were no spontaneous and piezoelectric polarization fields in the AlGaInP-based LEDs,³⁹ the slight red-shift of the emission peak was caused by the increased junction temperature because of Joule heating.^{40,41} In fact, a change in the maximum wavelength with a different injection current is undesirable for precise color control in display applications. Recently, a state-of-the-art growth technique for nonpolar or semipolar GaN LEDs was developed to reduce the peak shift.^{8,9} The ELOG of the LED over the reduced graphene oxide was also suggested to lower the junction temperature in MQWs.⁴² We also evaluated the full width at half-maximum (fwhm) of the emission peak to investigate the color purity. The fwhm value of the blue emission peak was 29.2 nm at an injection current of 5 mA and the fwhm of the yellow emission was 14.3 nm at 20 mA. This means that the LEDs have a high color purity compared with other light sources such as organic LEDs (OLEDs) that have FWHMs in the range of 50–200 nm.⁴³

Figure 3b shows the optical output power at different injection currents for both LEDs. The linear increase of the optical output power with the injection current ($L-I$) indicates that the emission intensity of each LED can be controlled to produce various colors. These attractive features of convenient color tunability and color purity of the LEDs would be very suitable for display applications. Finally, the typical rectifying characteristics in the current–voltage ($I-V$) curve, as shown in the inset of Figure 3b, and the linear behavior of the $L-I$ property imply that the LEDs were not thermally damaged during the bonding and transfer printing process.

Figure 4a shows the change in the color coordinates on the CIE $x-y$ chromaticity diagram with various injection currents into the yellow LED and at a constant injection current of 1 mA into the blue LED. As the injection current into the yellow LED increased from 3 mA to 15 mA in 3 mA increments, the color coordinate shifted from the blue to the yellow region. The gradual change in the position from (0.1812, 0.1860) to (0.4271, 0.3123) through the white coordinate of (0.3424, 0.2696) (corresponding to a correlated color temperature of 4634 K) at 9 mA indicates that color tuning was successfully controlled by the injection current. Figure 4b shows the EL spectra corresponding to the color coordinates in Figure 4a. It is notable that the EL intensity of the yellow LED can be controlled only by using the injection current into the yellow LED without any change in the EL intensity of the blue LED. This result clearly demonstrates the advantage of integrating different color LEDs on a single wafer, which can prevent any dependence of the color change on an external bias^{20,21} or efficiency loss due to down-conversion in phosphor-assisted white LEDs. Finally, a series of EL emission from a randomly selected LED pixel at various injection currents in the yellow LED is shown in Figure 4c. The independently operated yellow LED in the vertically stacked configuration shown in the upper images of Figure 4c has diverse mixed colors in the far-field as

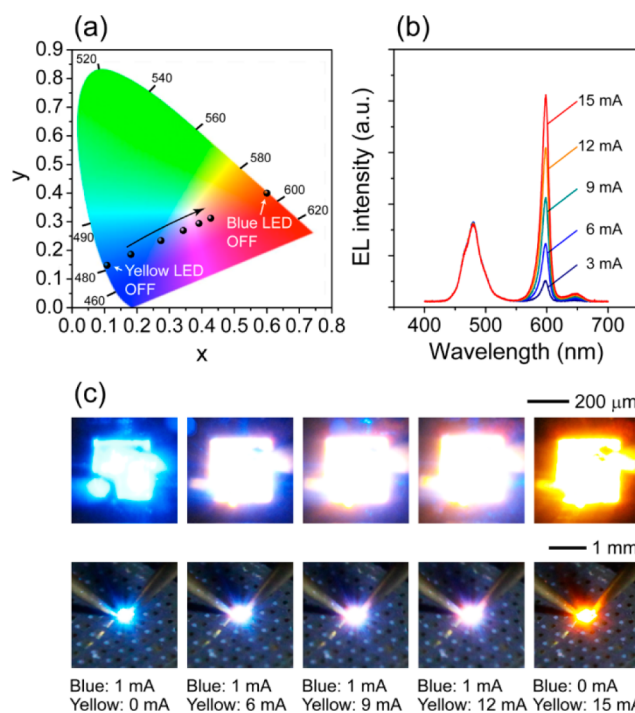


Figure 4. (a) Change in the color coordinate on a CIE $x-y$ chromaticity diagram. The injection current into the yellow LED was increased from 3 to 15 mA in 3 mA steps at a constant injection current of 1 mA in the blue LED. The additional two points are from the blue LED at 1 mA without yellow emission and the yellow LED at 15 mA without blue emission. (b) EL spectra corresponding to the color coordinates with an application of 3 mA to 15 mA injection current into the yellow LED while applying a fixed injection current of 1 mA in the blue LED. (c) Series of optical microscope images (upper line) and photographs (lower line) of the EL emission from a randomly selected LED pixel at various injection currents in the blue and yellow LEDs.

shown in the lower images of Figure 4c, confirming the efficacy of integrated LEDs for color tunability.

In conclusion, we investigate the ITO interlayer to vertically integrate GaN-based blue LEDs and AlGaInP-based yellow LEDs on a single substrate by using wafer bonding and transfer printing processes. EDX and TEM analysis show that the interdiffusion of In, O, and Ga and an amorphous layer at the interface between ITO and GaP enable the strong bonding of two heterogeneous optoelectronic materials. The successful EL emission and the color tunability show that this method is versatile and can be used to modulate a diverse range of colors in a stable manner. It is therefore feasible to generate polychromatic color emission by integrating different color LEDs in a vertically stacked configuration on a single substrate for various applications including high-resolution full-color displays, biomedical, and optogenetic systems.

■ ASSOCIATED CONTENT

Supporting Information

The epitaxial structure of GaN-based blue and the AlGaInP-based yellow LEDs, the chemical structure of the bonding interface, the detailed pixelation process of the vertically stacked LEDs, the EDX spectra of GaP and ITO surface before and after the bonding process, and the $I-V$ characteristics of the vertically stacked LEDs at high driving currents. This

material is available free of charge via the Internet at <http://pubs.acs.org>.

AUTHOR INFORMATION

Corresponding Author

*Prof. Seong-Ju Park. School of Materials Science and Engineering, Gwangju Institute of Science and Technology, Gwangju 500-712, Republic of Korea. E-mail address: sjpark@gist.ac.kr.

Notes

The authors declare no competing financial interest.

ACKNOWLEDGMENTS

This work was supported by the Industrial Strategic Technology Development Program (10041878), "Development of WPE 75% LED device process and standard evaluation technology", funded by the Ministry of Trade, Industry & Energy (MOTIE/KEIT).

REFERENCES

- (1) Pimputkar, S.; Speck, J. S.; DenBaars, S. P.; Nakamura, S. Prospects for LED Lighting. *Nat. Photonics* **2009**, *3*, 180–182.
- (2) Kim, J. K.; Schubert, E. F. Transcending the Replacement Paradigm of Solid-State Lighting. *Opt. Express* **2008**, *16*, 21835–21842.
- (3) Narukawa, Y.; Ichikawa, M.; Sanga, D.; Sano, M.; Mukai, T. White Light Emitting Diodes with Super-High Luminous Efficacy. *J. Phys. D: Appl. Phys.* **2010**, *43*, 354002.
- (4) Crawford, M. H. LEDs for Solid-State Lighting: Performance Challenges and Recent Advances. *IEEE J. Sel. Top. Quantum Electron.* **2009**, *15*, 1028–1040.
- (5) Tansu, N.; Zhao, H.; Liu, G.; Li, X.-H.; Zhang, J.; Tong, H.; Ee, Y.-K. III-Nitride Photonics. *IEEE Photonics J.* **2010**, *2*, 241–248.
- (6) Zhao, H.; Liu, G.; Zhang, J.; Poplawsky, J. D.; Dierolf, V.; Tansu, N. Approaches for High Internal Quantum Efficiency Green InGaN Light-Emitting Diodes with Large Overlap Quantum Wells. *Opt. Express* **2011**, *19*, A991–A1007.
- (7) Arif, R. A.; Ee, Y.-K.; Tansu, N. Polarization Engineering via Staggered InGaN Quantum Wells for Radiative Efficiency Enhancement of Light Emitting diodes. *Appl. Phys. Lett.* **2007**, *91*, 091110.
- (8) Feezell, D. F.; Speck, J. S.; DenBaars, S. P.; Nakamura, S. Semipolar (2021) InGaN/GaN Light-Emitting Diodes for High-Efficiency Solid-State Lighting. *J. Disp. Technol.* **2013**, *9*, 190–198.
- (9) Masui, H.; Nakamura, S.; DenBaars, S. P.; Mishra, U. K. Nonpolar and Semipolar III-Nitride Light-Emitting Diodes: Achievements and Challenges. *IEEE Trans. Electron Devices* **2010**, *57*, 88–100.
- (10) Cho, C.-Y.; Lee, S.-J.; Hong, S.-H.; Park, S.-C.; Park, S.-E.; Park, Y.; Park, S. J. Growth and Separation of High Quality GaN Epilayer from Sapphire Substrate by Lateral Epitaxial Overgrowth and Wet Chemical Etching. *Appl. Phys. Express* **2011**, *4*, 012104.
- (11) Kwon, M.-K.; Kim, J.-Y.; Kim, B.-H.; Park, I.-K.; Cho, C.-Y.; Byeon, C. C.; Park, S. J. Surface-Plasmon-Enhanced Light-Emitting Diodes. *Adv. Mater.* **2008**, *20*, 1253–1257.
- (12) Schnitzer, I.; Yablonovitch, E.; Caneau, C.; Gmitter, T. J.; Scherer, A. 30% External Quantum Efficiency from Surface Textured, Thin-Film Light-Emitting Diodes. *Appl. Phys. Lett.* **1993**, *63*, 2174–2176.
- (13) Kim, J.-Y.; Kwon, M.-K.; Lee, K.-S.; Park, S. J.; Kim, S. H.; Lee, K.-D. Enhanced Light Extraction from GaN-Based Green Light-Emitting Diode with Photonic Crystal. *Appl. Phys. Lett.* **2007**, *91*, 181109.
- (14) Jiang, H. X.; Jin, S. X.; Li, J.; Shaky, J.; Lin, J. Y. III-Nitride Blue Microdisplays. *Appl. Phys. Lett.* **2001**, *78*, 1303–1305.
- (15) Choi, H. W.; Jeon, C. W.; Dawson, M. D. Tapered Sidewall Dry Etching Process for GaN and Its Applications in Device Fabrication. *J. Vac. Sci. Technol. B* **2005**, *23*, 99–102.
- (16) Fan, Z. Y.; Lin, J. Y.; Jiang, H. X. III-Nitride Micro-Emitter Arrays: Development and Applications. *J. Phys. D: Appl. Phys.* **2008**, *41*, 094001.
- (17) Zhang, S.; Gong, Z.; McKendry, J. J. D.; Watson, S.; Cogman, A.; Xie, E.; Tian, P.; Gu, E.; Chen, Z.; Zhang, G.; Kelly, A. E.; Henderson, R. K.; Dawson, M. D. CMOS-Controlled Color-Tunable Smart Display. *IEEE Photonics J.* **2012**, *4*, 1639–1646.
- (18) Tchoe, Y.; Jo, J.; Kim, M.; Heo, J.; Yoo, G.; Sone, C.; Yi, G.-C. Variable-Color Light-Emitting Diodes Using GaN Microdonut Arrays. *Adv. Mater.* **2014**, *26*, 3019–3023.
- (19) Kim, T.-I.; McCall, J. G.; Jung, Y. H.; Huang, X.; Siuda, E. R.; Li, Y.; Song, J.; Song, Y. M.; Pao, H. A.; Kim, R.-H.; Lu, C.; Lee, S. D.; Song, I.-S.; Shin, G.; Al-Hasani, R.; Kim, S.; Tan, M. P.; Huang, Y.; Omenetto, F. G.; Rogers, J. A.; Bruchas, M. R. Injectable, Cellular-Scale Optoelectronics with Applications for Wireless Optogenetics. *Science* **2013**, *340*, 211–216.
- (20) Hong, Y. J.; Lee, C.-H.; Yoon, A.; Kim, M.; Seong, H.-K.; Chung, H. J.; Sone, C.; Park, Y. J.; Yi, G.-C. Visible-Color-Tunable Light-Emitting Diodes. *Adv. Mater.* **2011**, *23*, 3284–3288.
- (21) Gong, Z.; Liu, N. Y.; Tao, Y. B.; Massoubre, D.; Xie, E. Y.; Hu, X. D.; Chen, Z. Z.; Zhang, G. Y.; Pan, Y. B.; Hao, M. S.; Watson, I. M.; Gu, E.; Dawson, M. D. Electrical, Spectral and Optical Performance of Yellow-Green and Amber Micro-Pixelated InGaN Light-Emitting Diodes. *Semicond. Sci. Technol.* **2012**, *27*, 015003.
- (22) Wu, M.; Gong, Z.; Kuehne, A. J. C.; Kanibolotsky, A. L.; Chen, Y. J.; Perepichka, I. F.; Mackintosh, A. R.; Gu, E.; Skabara, P. J.; Pethrick, R. A.; Dawson, M. D. Hybrid GaN/Organic Microstructured Light-Emitting Devices via Ink-Jet Printing. *Opt. Express* **2009**, *17*, 16436–16443.
- (23) Black, A.; Hawkins, A. R.; Margalit, N. M.; Babić, D. I.; Holmes, A. L., Jr.; Chang, Y.-L.; Abraham, P.; Bowers, J. E.; Hu, E. L. Wafer Fusion: Materials Issues and Device Results. *IEEE J. Sel. Top. Quantum Electron.* **1997**, *3*, 943–951.
- (24) Zhu, Z.-H.; Ejeckam, F. E.; Qian, Y.; Zhang, J.; Zhang, Z.; Christenson, G. L.; Lo, Y. H. Wafer Bonding Technology and Its Applications in Optoelectronic Devices and Materials. *IEEE J. Sel. Top. Quantum Electron.* **1997**, *3*, 927–936.
- (25) Wong, W. S.; Kneissl, M.; Mei, P.; Treat, D. W.; Teepe, M.; Johnson, N. M. Continuous-Wave InGaN Multiple-Quantum-Well Laser Diodes on Copper Substrates. *Appl. Phys. Lett.* **2001**, *78*, 1198–1200.
- (26) Wong, W. S.; Sands, T.; Cheung, N. W.; Kneissl, M.; Bour, D. P.; Mei, P.; Romano, L. T.; Johnson, N. M. Fabrication of Thin-Film InGaN Light-Emitting Diode Membranes by Laser Lift-Off. *Appl. Phys. Lett.* **1999**, *75*, 1360–1362.
- (27) Kim, T.-I.; Jung, Y. H.; Song, J.; Kim, D.; Li, Y.; Kim, H.-S.; Song, I.-S.; Wierer, J. J.; Pao, H. A.; Huang, Y.; Rogers, J. A. High-Efficiency, Microscale GaN Light-Emitting Diodes and Their Thermal Properties on Unusual Substrates. *Small* **2012**, *8*, 1643–1649.
- (28) Chun, J.; Hwang, Y.; Choi, Y. S.; Jeong, T.; Baek, J. H.; Ko, H. C.; Park, S. J. Transfer of GaN LEDs from Sapphire to Flexible Substrates by Laser Lift-Off and Contact Printing. *IEEE Photonics Technol. Lett.* **2012**, *24*, 2115–2118.
- (29) Chun, J.; Hwang, Y.; Choi, Y. S.; Kim, J. J.; Jeong, T.; Baek, J. H.; Ko, H. C.; Park, S. J. Laser Lift-Off Transfer Printing of Patterned GaN Light-Emitting Diodes from Sapphire to Flexible Substrates Using a Cr/Au Laser Blocking Layer. *Scr. Mater.* **2014**, *77*, 13–16.
- (30) Liu, P.-C.; Hou, C.-Y.; Wu, Y.-S. Wafer Bonding for High-Brightness Light-Emitting Diodes via Indium Tin Oxide Intermediate Layers. *Thin Solid Films* **2005**, *478*, 280–285.
- (31) Murai, A.; Thompson, D. B.; Masui, H.; Fellows, N.; Mishra, U. K.; Nakamura, S.; DenBaars, S. P. Hexagonal Pyramid Shaped Light-Emitting Diodes Based on ZnO and GaN Direct Wafer Bonding. *Appl. Phys. Lett.* **2006**, *89*, 171116.
- (32) Moriceau, H.; Rieutord, F.; Fournel, F.; Tiec, Y. L.; Cioccio, L. D.; Morales, C.; Charvet, A. M.; Deguet, C. Overview of Recent Direct Wafer Bonding Advances and Applications. *Adv. Nat. Sci.: Nanosci. Nanotechnol.* **2010**, *1*, 043004.

(33) Youn, C. J.; Jeong, T. S.; Han, M. S.; Yang, J. W.; Lim, K. Y.; Yu, H. W. Influence of Various Activation Temperature on the Optical Degradation of Mg Doped InGaN/GaN MQW Blue LEDs. *J. Cryst. Growth* **2003**, *250*, 331–338.

(34) Kim, D. W.; Sung, Y. J.; Park, J. W.; Yeom, G. Y. A Study of Transparent Indium Tin Oxide Contact to p-GaN. *Thin Solid Films* **2001**, *398*, 87–92.

(35) Choi, J.-H.; Jang, S.-H.; Jang, J.-S. Electrical, Optical, and Structural Characteristics of Ohmic Contacts between p-GaN and ITO Deposited by DC- and RF-Magnetron Sputtering. *Electron. Mater. Lett.* **2013**, *9*, 425–428.

(36) Zhang, Y.; Guo, W.; Gao, W.; Li, C.; Ding, T. Properties of the ITO Layer in a Novel Red Light-Emitting Diode. *J. Semicond.* **2010**, *31*, 043002.

(37) Jung, Y.; Wang, X.; Kim, J.; Kim, S. H.; Ren, F.; Pearton, S. J.; Kim, J. GaN-Based Light-Emitting Diodes on Origami Substrates. *Appl. Phys. Lett.* **2012**, *100*, 231113.

(38) Gong, Z.; Jin, S.; Chen, Y.; McKendry, J.; Massoubre, D.; Watson, I. M.; Gu, E.; Dawson, M. D. Size-Dependent Light Output, Spectral Shift, and Self-Heating of 400 nm InGaN Light-Emitting Diodes. *J. Appl. Phys.* **2010**, *107*, 013103.

(39) Shim, J.-I.; Han, D.-P.; Kim, H.; Shin, D.-S.; Lin, G.-B.; Meyaard, D. S.; Shan, Q.; Cho, J.; Schubert, E. F.; Shim, H.; Sone, C. Efficiency Droop in AlGaInP and GaInN Light-Emitting Diodes. *Appl. Phys. Lett.* **2012**, *100*, 111106.

(40) Chhajed, S.; Xi, Y.; Li, Y.-L.; Gessmann, Th.; Schubert, E. F. Influence of Junction Temperature on Chromaticity and Color-Rendering Properties of Trichromatic White-Light Sources Based on Light-Emitting Diodes. *J. Appl. Phys.* **2005**, *97*, 054506.

(41) Manninen, P.; Orreveläinen, P. On Spectral and Thermal Behaviors of AlGaInP Light-Emitting Diodes under Pulse-Width Modulation. *Appl. Phys. Lett.* **2007**, *91*, 181121.

(42) Han, N.; Cuong, T. V.; Han, M.; Ryu, B. D.; Chandramohan, S.; Park, J. B.; Kang, J. H.; Park, Y.-J.; Ko, K. B.; Kim, H. Y.; Kim, H. K.; Ryu, J. H.; Katharria, Y. S.; Choi, C.-J.; Hong, C.-H. Improved Heat Dissipation in Gallium Nitride Light-Emitting Diodes with Embedded Graphene Oxide Pattern. *Nat. Commun.* **2013**, *4*, 1452.

(43) O'Riordan, A.; O'Connor, E.; Moynihan, S.; Llinares, X.; Deun, R. V.; Fias, P.; Nockemann, P.; Binnemans, K.; Redmond, G. Narrow Bandwidth Red Electroluminescence from Solution-Processed Lanthanide-Doped Polymer Thin Films. *Thin Solid Films* **2005**, *491*, 264–269.